Available online at www.sciencedirect.com
ScienceDirect
International Journal of Mass Spectrometry 266 (2007) 129–137
International Journal of Mass Spectrometry
www.elsevier.com/locate/ijms

Artifacts of MALDI sample preparation investigated by high-resolution scanning microprobe matrix-assisted laser desorption/ionization (SMALDI) imaging mass spectrometry

Werner Bouschen, Bernhard Spengler *

Institute of Inorganic and Analytical Chemistry, Justus Liebig University of Giessen, Schubertstr. 60, D-35392 Giessen, Germany

Received 12 June 2007; received in revised form 15 July 2007; accepted 17 July 2007
Available online 2 August 2007

Abstract

MALDI dried droplet preparations using 2,5-dihydroxybenzoic acid as a matrix were investigated by scanning microprobe matrix-assisted laser desorption/ionization mass spectrometry (SMALDI MS). Mass spectrometric images of lateral distributions of sample components and impurities were obtained with a lateral resolution of 1 μm. Results show the crystallization behavior of the matrix as a function of various physico-chemical parameters as well as inhomogeneous separation of components on various scales between millimeters and sub-micrometers. Segregation was found to be a sample-wide, crystal-wide and sub-crystalline, general phenomenon. Effective parameters in this context are hydrophobicity, polarity, and mobility, among others. Peptide ion signals were observed from inside the matrix crystals, while carbohydrate signals and alkali ion signals were observed predominantly from outside the larger matrix crystals.

The described investigations shed some light on processes that cause well-known problems of quantification and sample suppression in MALDI MS. They also help to optimize matrix preparation for high-resolution MALDI imaging of biological samples.

Keywords: SMALDI MS; Imaging mass spectrometry; MALDI preparation; Quantification; Peptide

1. Introduction

The preparation of MALDI samples and likewise the generation of ions in the MALDI process are still poorly understood phenomena despite the intense use of the method in routine laboratory work. The desorption/ionization process is still the subject of extensive investigations [1–6]. Following the introduction of MALDI by Karas et al. [7], significant improvements in preparation techniques, matrix application [8–10] and instrumental developments [11], enhanced the analysis of biological compounds and diagnostics of diseases [12–15]. Preparation protocols for MALDI are well described in the literature [16,17], but still there are mysteries about individual handling procedures in achieving optimized results with respect to sensitivity and quantification. Different matrices are required for different analyte classes and matrix/analyte parameters have to be optimized individually. After employing these individual preparation protocols, the matrix is typically inhomogeneously distributed due to the essential matrix crystallization process. The size of growing crystals can vary between a few μm and 500 μm. The speed of matrix crystallization [18] and the choice of solvent [19] both have a significant influence on the crystal growth. Inhomogeneity is on the one hand a function of the matrix crystal size. Very little is known so far, on the other hand, about inhomogeneity of the analyte distribution within individual crystals.

Instrumentation for high-resolution scanning microprobe MALDI (SMALDI) mass spectrometry presented by our group [20] enables us to examine the distribution of components in MALDI samples with a lateral resolution of about 1 μm. SMALDI-MS is the first technique to obtain label-free molecular information about processes connected to crystallization of the matrix with this lateral resolution. Results described in the following will help to enhance preparation techniques for quantitative and highly sensitive MALDI analysis in general. Furthermore, MALDI imaging and especially high lateral resolution SMALDI imaging [21,22] will benefit from these studies,

* Corresponding author.
E-mail addresses: Werner.Bouschen@uni-giessen.de (W. Bouschen), Bernhard.Spengler@uni-giessen.de (B. Spengler).
URL: http://www.uni-giessen.de/analytik/ (B. Spengler).

1387-3806/$ – see front matter © 2007 Elsevier B.V. All rights reserved.
doi:10.1016/j.ijms.2007.07.017

as migration and segregation phenomena in biological studies are better understood on the low μm scale. Finally, minimizing migration is the key parameter for improving lateral resolution of imaging techniques.

In the present study we show that migration and segregation of analytes in a standard preparation play an important role in obtaining representative mass spectra of complex mixtures. Strategies for homogenous sample preparation were found to improve MALDI analysis in terms of identification and quantification of compounds. In imaging mass spectrometry, on the other hand, an optimized homogenous matrix application allows to image the sample in a way, which is more representative for the original distribution.

2. Experimental

2.1. Instrumentation

The dedicated instrument 'Lamma 2000' is described elsewere[20]. A nitrogen laser at 337 nm wavelength with a laser beam focused to 0.7 μm was used for high-resolution imaging of analyte distributions. Images represent an area of 100 μm × 100 μm of the scanned surface obtained with a step size of 1 μm. Concentration distribution images were produced for sample components up to $m/z = 6200$ u. Subsequently 10,000 mass spectra per imaging set were acquired and evaluated automatically by dedicated software developed in-house. No mass signals needed to be selected prior to SMALDI mass spectrometry. Color table images were produced by standard graphical software. Every RGB pixel represents the signal intensities for up to three selected masses. All mass spectra were acquired from a single laser pulse per sample position. The instrument was working in the linear positive-ion mode at an acceleration voltage of 13 kV.

2.2. Material

For the study of migration phenomena, mixtures of several peptides and an oligosaccharide were investigated (Table 1). 2,5-Dihydroxybenzoic acid (DHB) was used as a matrix for MALDI preparation.

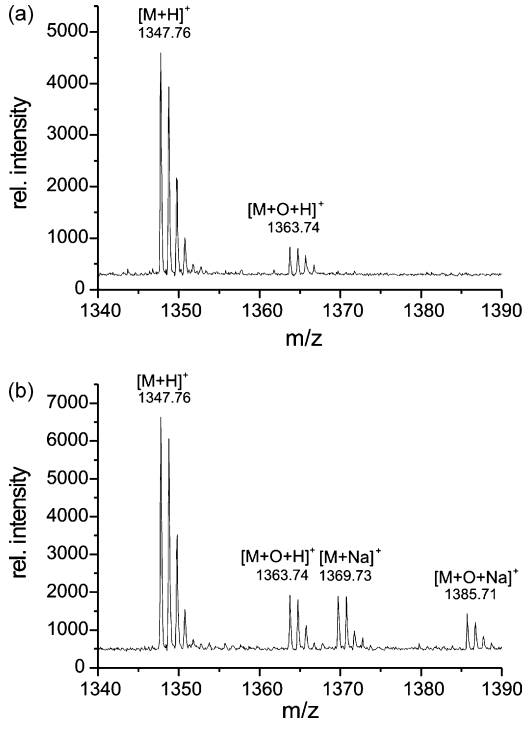

Fig. 1. Comparison between rim (a) and inner region (b) of a dried droplet preparation. Sodium-attached peptide ions were observed predominantly from the inner region.

Solvents of highest quality (Aceton, ACS Merck, Darmstadt, Germany; Isopropanol, Licrosolv Merck, Darmstadt, Germany; Water, ACS Sigma–Aldrich, Frankfurt, Germany; Ethanol, Uvasol Merck, Darmstadt, Germany; TFA, Fluka Riedel-de Haen, Taufkirchen, Germany) were used for dissolving the analytes and for cleaning the target prior to preparation.

2.3. Sample preparation

A standard MALDI preparation protocol was employed to investigate possible correlations between crystallization of the matrix and migration or segregation of analytes.

Dried droplet preparation [24] led to circular crystallized samples with diameters of approximately two millimeters. The

Table 1
List of peptides and oligosaccharide used for the study

Name	$M_{monoisot.}$ (u)	B&B index	p*I*	Company
Cellotriose (*O*-β-D-glucopyranosyl-(1→4)-*O*-β-D-glucopyranosyl-(1→4)-D-glucose)	504.168	–	–	Sigma–Aldrich Frankfurt Germany
Vasopressin[Arg^8] (H–CYFQNCPRG–NH_2)	1085.454	960 (hydrophilic)	5.2	Bachem AG Weil am Rhein, Germany
Dynorphin 1–9 (H–YGGFLRRIR–OH)	1136.657	−2360 (hydrophobic)	12.2	Bachem AG Weil am Rhein, Germany
Lipotropin 1-10 (H–ELAGAPPEPA–OH)	950.471	1500 (hydrophilic)	3.18	Bachem AG Weil am Rhein, Germany
Anti-inflammatory peptide (H–HDMNKVLDL–OH)	1083.538	−1450 (hydrophobic)	5.12	Bachem AG Weil am Rhein, Germany
Substance P (H–RPKPQQFFGLM–NH_2)	1346.728	−1790 (hydrophobic)	11.51	Sigma–Aldrich Frankfurt, Germany
Melittin (H–GIGAVLKVLTTGLPA LISWIKRKRQQ–NH_2)	2844.754	−4470 (hydrophobic)	12.53	Serva Electrophoresis Heidelberg, Germany
Human insulin A chain: H–GIVEQCCTSICSLY QLENYCN–OH B Chain: H–FVNQHLCGSHLVE ALYLVCGERGFFYTPKT–OH)	5803.638	−7960 (hydrophobic)	5.32	Sigma–Aldrich Frankfurt, Germany

B&B index [23] is included as a hydrophobicity parameter.

rim of this sample consisted of larger crystals (typically less than 200 μm) and its inner region was composed of fine crystals (typically less than 5 μm). Prior to sample preparation the sample holders were cleaned intensely in order to avoid contamination of the sample. Cleaning was repeated several times with different solvents (acetone, isopropanol, water and ethanol) and the sample holders were dried in between with a dust free ultraclean wipe. Finally, sample holders were moistened with ethanol and dried under a hot, filtered air flow. A volume of 1 μl of a peptide mixture (concentrations: 5×10^{-5} mol/l in ethanol/water (1:1)) was dripped on the still warm sample plate. Afterwards 1 μl DHB solution (20 mg/ml in 60:40 ethanol/0.1% aqueous TFA) was added to the droplet and mixed on target by successively drawing up the mixture in a pipette tip and redripping it. Depending on the desired duration of the crystallization procedure, the sample was dried either in room air within several minutes or under a hot air flow in a few seconds. The final size of the growing crystals was found to be strongly depending on the speed of drying, as expected. A pronounced rim of the sample was formed if the sample plate was dried slowly in air. It consisted of large, up to several 100 μm long, crystals. By increasing the amount of water in the matrix solution this effect could be enhanced due to the substantially lower vapor pressure of water versus ethanol. Since the inner region of the sample is typically still covered with liquid during crystallization of the rim, the small crystals in this part form just shortly before the complete sample dries up. Within seconds during the final drying procedure, many very small crystals are formed in the inner region. This layer can be distinguished clearly from the rim of the sample, usually by a narrow region which is almost free of sample material and matrix. Images were acquired from the rim and from the inner region of the dried droplet.

3. Result and discussion

3.1. Segregation within dried droplet sample

It was observed in this study that sample components considerably separated during crystallization of the matrix. When comparing mass spectra from the rim and from the inner region of the sample, a localization of alkali salt contaminations predominantly in the inner region was found (Fig. 1). This

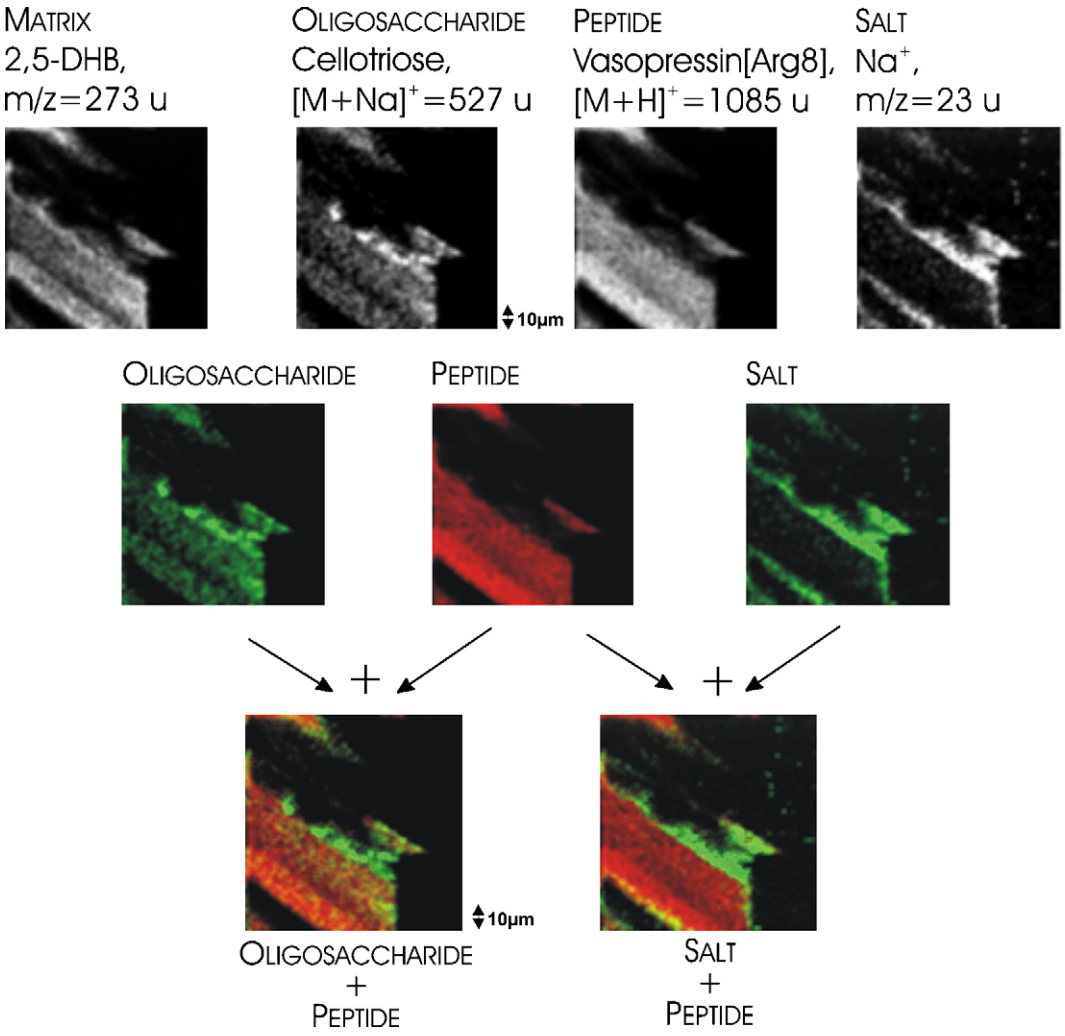

Fig. 2. SMALDI MS images of matrix DHB, cellotriose, vasopressin and sodium. Sampled area was 100 μm × 100 μm, scanning step size was 1 μm. (First row) Gray scale distribution images. (Second row) Colored distribution images. (Third row) Red/green overlay images.

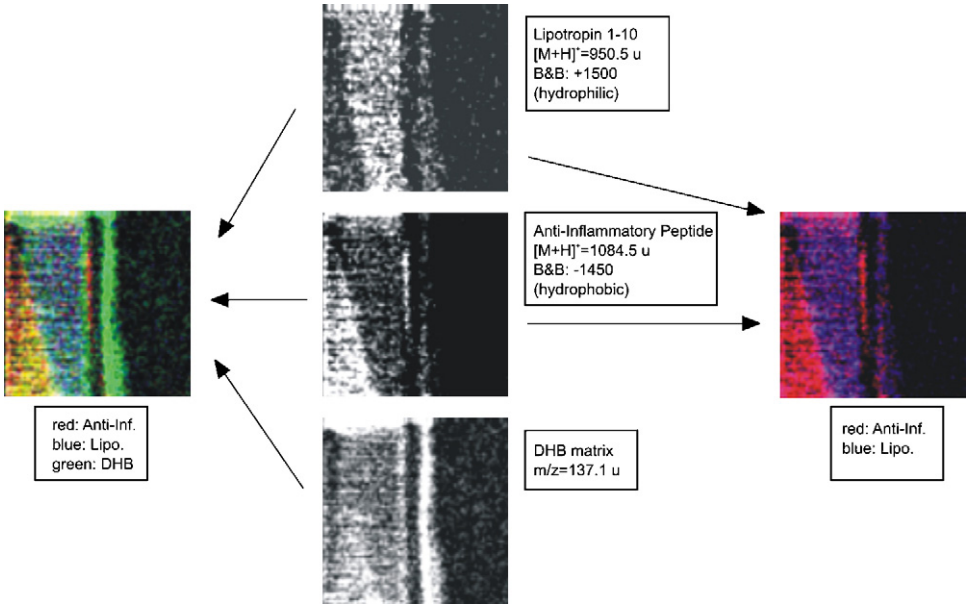

Fig. 3. SMALDI images of mixtures of highly hydrophilic lipotropin 1–10 and highly hydrophobic anti-inflammatory peptide in DHB matrix, using a slowly crystallizing dried-droplet preparation. (Middle) Gray scale distribution images, scanned area 100 μm × 100 μm, step size 1 μm. (Left) Combination of all three gray scale images. (Right) Combination of lipotropin1–10 and anti-inflammatory peptide.

observation can be explained by the fact that (positively charged) alkali ions remain solved in the polar solvents (ethanol/water) during crystallization of the rim, rather than being incorporated in the matrix crystals. Only with the final drying of the inner region, alkali salts precipitate.

The same effect was observed on the micrometer scale as well. Fig. 2 shows a SMALDI image of a peptide/carbohydrate mixture, acquired with a scanning step size of 1 μm for an image area of 100 μm times 100 μm. A dried droplet preparation (as described above) of cellotriose and of the hydrophobic peptide vasopressin[arg8] was mixed on the sample holder. The sample was subsequently dried under a warm air flow within approximately 1 min. Alkali ions were present as impurities only.

The upper row of the figure shows gray scale images of the matrix DHB, the carbohydrate cellotriose, of the peptide vasopressin and of sodium ions. In the second row, carbohydrate, peptide and sodium ion images are colored in green and red, and are finally combined in two red/green images in the third row.

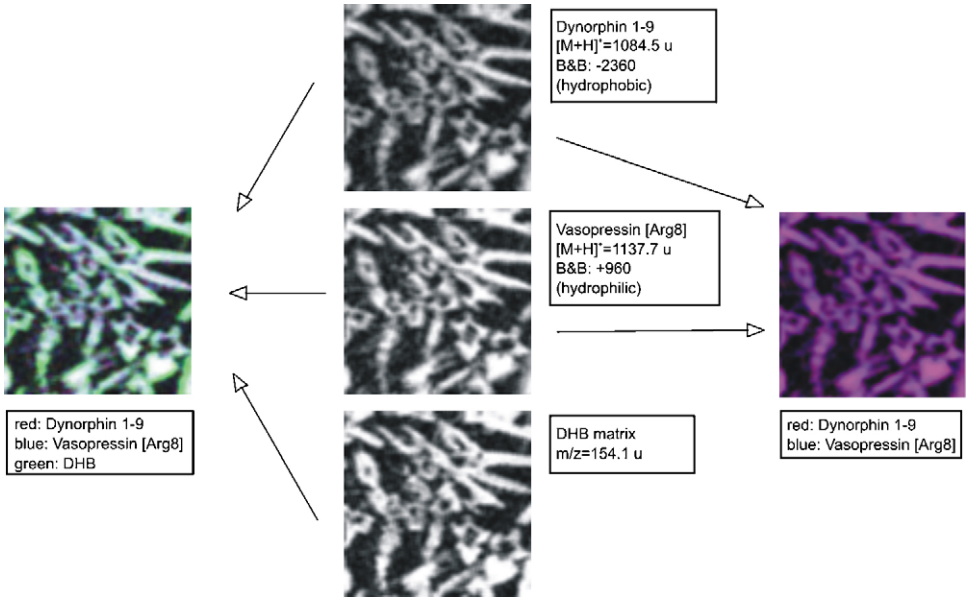

Fig. 4. SMALDI images of mixtures of highly hydrophilic vasopressin[arg8] and highly hydrophobic dynorphin 1–9 in DHB matrix, using a rapid crystallizing dried-droplet preparation. (Middle) Gray scale distribution images, scanned area 100 μm × 100 μm, step size 1 μm. (Left) Combination of all three gray scale images. (Right) Combination of vasopressin[arg8] and dynorphin 1–9.

A separation of components was observed, probably driven by their hydrophobicity and/or polarity values. The ion distribution images show a large matrix crystal (larger than the dimension of the image) with incorporated vasopressin in red. Sodium ions (green) were obtained from outside and from the surface of this crystal only. This again shows that sodium ions remain in solution until complete drying, while matrix crystals already formed. Due to similar hydrophobicity and polarity of matrix and peptides, the latter are incorporated in the forming matrix crystals. Carbohydrates (green), on the other hand, have a higher polarity than peptides and have a high affinity to alkali ions. They have thus a lower tendency to co-crystallize with the matrix. As a result carbohydrate signals were obtained from outside the matrix crystals, and in co-localization with alkali ions.

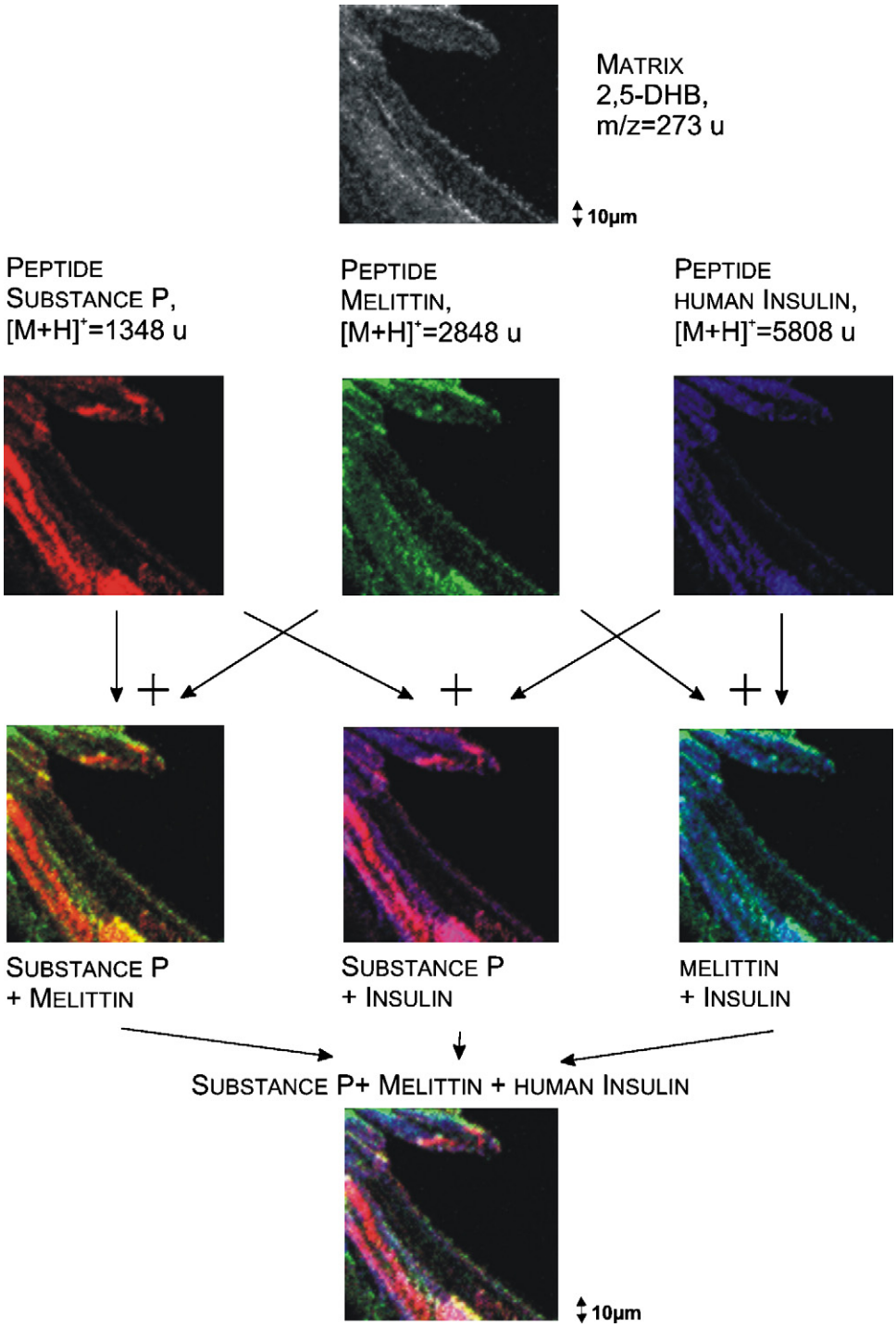

Fig. 5. SMALDI images from the rim of a dried droplet preparation of a peptide mixture. (First and second rows) Distribution images of DHB matrix, substance P, melittin and human insulin. Scanned area was 100 μm × 100 μm, step size was 1 μm. (Third and fourth rows) RGB overlay images.

3.2. Segregation within matrix crystals

Besides separation of components within the dried droplet sample, additional sample inhomogeneities were observed within individual matrix crystals. The speed of crystallization was found to be a key parameter in this respect. Fig. 3 describes the investigation of a peptide mixture, consisting of the strongly hydrophilic lipotropin 1–10 and the strongly hydrophobic anti-inflammatory peptide. Again a dried droplet preparation was used as described. The sample crystallized without artificial air flow within approximately 5 min at room temperature. The slow crystallization process resulted in large DHB crystals with a size of up to 500 μm at the rim of the sample. The gray scale images (Fig. 3) of the scanned area show homogeneous signal intensities from the matrix molecule DHB across the complete crystal, while completely different distributions were found of the two peptides within one large matrix crystal. The left part of the images is dominated by a matrix crystal which is larger

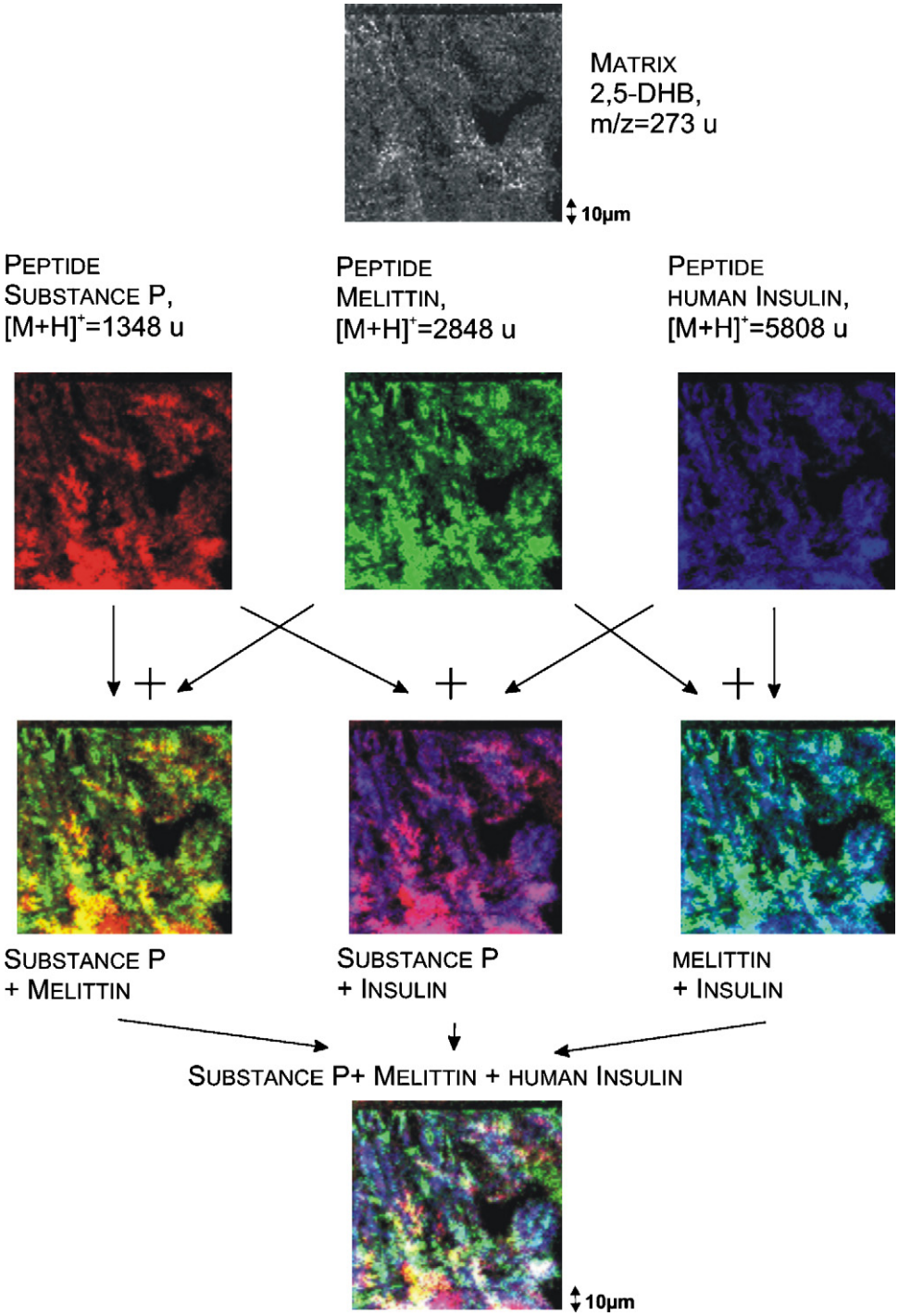

Fig. 6. SMALDI images from the inner region of the same sample as in Fig. 5. (First and second rows) Distribution images of DHB matrix, substance P, melittin and human insulin. Scanned area was 100 μm × 100 μm, step size was 1 μm. (Third and fourth row) RGB overlay images.

than the scanned area. In the center a narrow matrix needle with a width of approximately 10 μm is to be seen. In the large crystal the hydrophilic peptide lipotropin dominates the upper right part, while the hydrophobic anti-inflammatory peptide is mainly found in the lower left region. This becomes particularly obvious, when in an RGB color palette image the blue channel is assigned to the signal intensity of lipotropin and the red channel to the signal intensity of anti-inflammatory peptide. A clear segregation of the two analytes is thus found, most probably driven by the strong differences in hydrophobicity. This segregation of the two peptides can also be demonstrated by combining all three gray scale images including the matrix signal. This hydrophobicity-driven segregation behavior cannot be explained at the moment. Possible reasons are self-assembly effects, formation of a two-phase system when the water/ethanol mixture dries down, or different crystal modifications leading to different incorporation behavior for hydrophobic and hydrophilic dopants.

In contrast to the described behavior, a faster matrix crystallization procedure led to much weaker segregation effects. In Fig. 4, SMALDI images of a peptide mixture of dynorphin 1–9 (hydrophobic) and vasopressin[Arg8] (hydrophilic) are shown. Concentrations were the same as used for Fig. 3. After mixing analyte and matrix solutions on a preheated target, the liquid was quickly dried with a hot air flow. A very fast drying and crystallization within approximately 5–10 s can be achieved by this procedure. The resulting matrix crystals are substantially smaller than those produced by slow crystallization. The gray scale images of the scanned area of 100 μm × 100 μm show the distribution of the two analytes and the matrix (Fig. 4, middle). Within the crystals, having sizes of 10–50 μm, the two peptides were found to be almost homogeneously distributed. The colored image on the right shows mainly violet (red plus blue) crystal areas rather than separated blue or red regions, indicating a strongly reduced segregation behavior under fast crystallization conditions. By including the third component (matrix: green) in an RGB image, the crystals appear mostly white, indicating similar intensities of all three color channels. Stronger matrix signals (green) were observed from the rim of the small crystals.

3.3. Segregation of similar peptides

Peptides with less pronounced differences in hydrophobicity and polarity still express considerable segregation behavior. Peptides substance P, melittin and human insulin were investigated, all three having negative Bull and Breeze indices (hydrophobic peptides) but differ in mass and thus in molecular mobility in solution. The isoelectric points of the three peptides are 11.51 (substance P), 12.53 (melittin), and 5.32 (human insulin).

A dried droplet preparation of a mixture of the peptides (5×10^{-5} mol/l substance P, 1×10^{-4} mol/l melittin, 2×10^{-4} mol/l human insulin) was used. Aliquots of 0.5 μl of the peptide mixture and 0.5 μl of the matrix solution were mixed on the sample holder and dried under a warm air flow within approximately 1 min.

The prepared samples showed a rim of large crystals and a fine-crystalline inner region. An area of 100 μm × 100 μm was scanned with a step size of 1 μm.

Fig. 5 shows SMALDI images obtained from the rim, indicating a strong inhomogeneous distribution of the analyte components. While substance P is predominantly located in the left part of the imaged crystal, melittin is located more in the central part of the crystal. Human insulin, in contrast to that, shows the most homogeneous distribution of the three peptides. This can be explained by the increased mobility of the small peptide substance P compared to the larger peptide insulin. Chaotic transportation and liquid flow processes during drying and crystallization will have a stronger displacement effect on the more mobile components, compared to the less mobile components.

Fig. 6 confirms this observation for the inner region. No inhomogeneities within the fine crystals were resolved, but segregation of analyte components at different locations of the inner region was found.

The observed effects of analyte segregation during matrix crystal formation are in contrast to earlier observations of Horneffer et al. [25]. In that investigation, confocal images of fluorescently labeled proteins in DHB matrix crystals had shown a homogeneous distribution within the crystals. These results cannot be directly compared to our data, however, because doped crystals for confocal microscopy were grown very slowly from a chemical equilibrium and to a much larger size.

4. Conclusion

The described investigations clearly demonstrate that migration and segregation play an important role in MALDI sample preparation. Scanning microprobe MALDI mass spectrometry (SMALDI MS) was shown to be an excellent method to investigate such phenomena. Distributions of analytes both within the sample and within the individual matrix crystals depend on several factors. Alkali ions were detected almost exclusively from outside the matrix crystals and predominantly from the inner fine-crystalline region of a dried sample. Speed of crystallization was found to have a strong effect on migration and segregation processes. Rapid crystallization to small crystals, as shown in Fig. 4, leads to a nearly homogeneous analyte distribution within the available lateral resolution. Furthermore, analyte parameters such as hydrophobicity, polarity, mass and mobility in solution obviously play a major role for such phenomena. It was found that analyte components that differ strongly in at least one of these parameters, might segregate strongly within crystals. At least for smaller peptides, high mobility in solution can lead to intense movements within the chaotic flow during sample drying.

Accuracy of quantification was recognized earlier as being rather limited in MALDI MS [26–28]. The above investigations are able to explain why both, absolute and relative quantification in MALDI MS are problematic. Migration and segregation of analyte components were shown to cause inhomogeneous concentration levels on the millimeter, micrometer and probably sub-micrometer scale. These lateral concentration variations inevitably result in large shot-to-shot variations of signal intensi-

ties, pure linearity of signal intensities with concentrations, and analyte suppression effects.

Suppression of analyte signal in this context can be understood as a result not only of analyte basicity and charge competition, but also of parameters such as solubility in solvent mixtures, analyte mobility, surface activity and co-crystallization enthalpy. The ion signal of a second peptide component might be suppressed, for example, because co-crystallization sites in matrix crystals are already occupied by a first peptide component, having a lower co-crystallization enthalpy.

The size of inomogeneities relative to the size of the laser spot has an effect on the quantifyability of signal data. A large laser spot will integrate and average over a large area of very different local concentrations, while a small laser spot is able to image these local concentrations (as shown in this paper) with a reasonable accuracy of relative quantification. Nevertheless, shot-to-shot variations will still dominate even with large laser spots due to inhomogeneities in *z*-direction of the sample (depth profile).

The described SMALDI investigations of dried droplet preparations clearly illustrate that matrix preparation is an efficient sample-cleaning step. In this context, migration and segregation of components has to be interpreted as an extremely advantageous phenomenon of MALDI. The complementary distribution of vasopressin[arg8] and sodium ions in Fig. 2 indicates, that alkali ions are excluded from growing matrix crystals, while peptides are incorporated. This explains the high tolerance of MALDI versus salt impurities [29], in comparison to other ionization techniques such as electrospray ionization (ESI).

Strategies for an optimized MALDI preparation therefore have to find a compromise between homogeneous distribution of analyte components (rapid crystallization) and salt exclusion (slow crystallization). Crystallization speed and behavior can be modified for example by heating the sample holder, by a suitable choice of solvent mixtures, by modifying the viscosity of sample solutions or by varying the morphology, hydrophobicity and material of the sample holder surface. Reduced salt exclusion is especially a problem with dedicated high-resolution matrix preparation techniques [21] which are necessary for achieving lateral resolutions in SMALDI imaging MS in the micrometer range. Smaller matrix crystals are known to reduce analytical sensitivity of MALDI considerably. Optimization of biological SMALDI sample preparation then has to aim at not only minimized crystal size and minimized analyte migration, but also sample purity with respect to ionic components.

Acknowledgements

Financial support by the European Union (LSHG-CT-2005-518194) and by the Bundesministerium für Bildung und Forschung (NGFN-2, 0313442) is gratefully acknowledged.

References

[1] V. Bökelmann, B. Spengler, R. Kaufmann, Dynamical parameters of ion ejection and ion formation in matrix-assisted laser desorption/ionisation, Eur. J. Mass Spectrom. 1 (1995) 81.

[2] B. Spengler, D. Kirsch, On the formation of ion velocities in matrix-assisted laser desorption ionization: virtual desorption time as an additional parameter describing ion ejection dynamicy, Int. J. Mass Spectrom. 226 (2003) 71.

[3] R. Knochenmuss, R. Zenobi, MALDI ionization: the role of in-plume processes, Chem. Rev. 103 (2003) 441.

[4] M. Karas, M. Glückmann, J. Schäfer, Ionization in matrix-assisted laser desorption/ionization: singly charged molecular ions are the lucky survivors, J. Mass Spectrom. 35 (2000) 1.

[5] J. Kampmeier, M. Schürenberg, K. Dreisewerd, K. Strupat, K. Strupat, J. Kampmeier, V. Horneffer, Investigation of 2,5-DHB and succinic acid as matrices for UV an IR MALDI. Part I. UV and laser ablation in the MALDI process, Int. J. Mass Spectrom. Ion Process. 169 (1997) 31.

[6] K. Strupat, J. Kampmeier, V. Horneffer, Investigation of 2,5-DHB and succinic acid as matrices for UV an IR MALDI. Part II. Crystallographic and mass spectrometric analysis, Int. J. Mass Spectrom. Ion Process. 169 (1997) 43.

[7] M. Karas, D. Bachmann, U. Bahr, F. Hillenkamp, Matrix-assisted ultraviolet laser desorption of non-volatile compounds, Int. J. Mass Spectrom. Ion Process. 78 (1987) 53–68.

[8] K. Strupat, M. Karas, F. Hillenkamp, 2,5-Dihydroxybenzoic acid: a new matrix for laser desorption-ionisation mass spectrometry, Int. J. Mass Spectrom. Ion Process. 111 (1991) 89.

[9] R.C. Beavis, B.T. Chait, Cinnamic acids derivatives as matrices for ultraviolet laser desorption mass spectrometry of proteins, Rapid Commun. Mass Spectrom. 3/12 (1989) 432.

[10] R.C. Beavis, T. Chaudhary, B.T. Chait, Alpha-cyano-4-hydroxycinnamic acid as a matrix for matrix-assisted laser desorption mass spectrometry, Org. Mass Spectrom. 27 (1992) 156.

[11] R.C. Beavis, B.T. Chait, K.G. Standing, Matrix-assisted laser-desorption mass spectrometry using 355 nm radiation, Rapid Commun. Mass Spectrom. 3 (1989) 436.

[12] T. Flad, B. Spengler, H. Kalbacher, P. Brossart, D. Baier, R. Kaufmann, P. Bold, S. Metzger, M. Blüggel, H.E. Meyer, B. Kurz, C.A. Müller, Direct identification of major histocompatibility complex class I-bound tumor-associated peptide antigens of a renal carcinoma cell line by a novel mass spectrometric method, Cancer Res. 58 (1998) 5803.

[13] G. Porcellati, in: L.A. Horrocks (Ed.), Phospholipids in Nervous Systems, 1, [Hrsg] Raven Press, New York, 1985.

[14] M. Söderberg, C. Edlund, I. Alafuzoff, K. Kristenson, G.J. Dallner, Lipid composition in different regions of the brain in Alzheimer's disease/senile dementia of Alzheimer type, J. Neurochem. 59 (1992) 1646.

[15] T. Klein, D. Kirsch, R. Kaufmann, D. Riesner, Prion rods contain small amounts of two host spingolipids as revealed by thin-layer chromatography and mass spectrometry, Biol. Chem. 379 (1998) 655.

[16] L.M. Preston, K.K. Murray, D.H. Russell, Reproducibility and quantitation of matrix-assisted laser desorption ionization mass spectrometry: effects of nitrocellulose on peptide ion yields, Biol. Mass Spectrom. 22 (9) (1993) 544.

[17] J. Gobom, E. Nordhoff, E. Mirgorodskaya, R. Ekmann, P. Roepstorff, Sample purification and preparation technique based on nano-scale reversed-phase columns for the sensitive analysis of complex peptide mixtures by matrix-assisted laser desorption/ionization mass spectrometry, J. Mass Spectrom. 34 (1999) 105.

[18] O. Vorm, P. Roepstorff, M. Mann, Improved resolution and very high sensitivity in MALDI TOF of matrix surfaces made by fast evaporation, Anal. Chem. 66 (1994) 3281.

[19] Talat S Yalcin, Yuqin S Dai, Li Liang, Matrix-assisted laser desorption/ionization time-of-flight mass spectrometry for polymer analysis: solvent effect in sample preparation, J. Am. Soc. Mass Spectrom. 9–12 (1998) 1303.

[20] B. Spengler, M. Hubert, Scanning microprobe matrix-assisted laser desorption ionization (SMALDI) mass spectrometry: Instrumentation for sub-micrometer resolved LDI and MALDI surface analysis, J. Am. Soc. Mass Spectrom. 13 (2002) 735.

[21] W. Bouschen, O. Schulz, D. Eikel, B. Spengler, Preparation techniques in high-resolution imaging using Scanning Microprobe MALDI mass spectrometry (SMALDI-MS), in preparation.

[22] W. Bouschen, B. Spengler, SMALDI imaging at 1 μm lateral resolution (Extended Abstract), in: Proceedings of the 52nd ASMS Conference on Mass Spectrometry and Allied Topics, Nashville, USA, May 23–27, 2004.
[23] H.B. Bull, K. Breese, Surface tension of amino acid solutions: a hydrophobicity scale of the amino acid residues, Arch. Biochem. Biophys. 161 (1974) 665.
[24] M. Karas, F. Hillenkamp, Laser desorption ionization of proteins with molecular masses exceeding 10000 Daltons, Anal. Chem. 60 (1988) 2299.
[25] V. Horneffer, A. Forsmann, K. Strupat, F. Hillenkamp, U. Kubitscheck, Localization of analyte molecules in MALDI preparations by confocal laser scanning microscopy, Anal. Chem. 73 (2001) 1016.
[26] J.R. Perkins, B. Smith, R.T. Gallagher, D.S. Jones, S.C. Davis, A.D. Hoffmann, K.B. Tomer, Application of electrospray mass spectrometry and matrix-assisted laser desorption ionization time-of-flight mass spectrometry for molecular weight assignment of peptides in complex mixtures, J. Am. Soc. Mass Spectrom. 4 (1993) 670.
[27] T.M. Belleci, J.T. Stults, Tryptic mapping of recombinant proteins by matrix-assisted laser desorption/ionization mass spectrometry, Anal. Chem. 65 (1993) 1709.
[28] M.Z. Wang, M.C. Fitzgerald, A solid sample preparation method that reduces signal suppression effects in the MALDI analysis of peptides, Anal. Chem. 73 (2001) 625.
[29] B. Spengler, Postsource decay analysis in matrix-assisted laser desorption ionisation mass spectrometry of biomolecules, J. Mass Spectrom. 32 (1997) 1019.